ORIGINAL ARTICLE

Wide beam reconstruction for half-dose or half-time cardiac gated SPECT acquisitions: optimization of resources and reduction in radiation exposure

Claudio Marcassa · Riccardo Campini · Orazio Zoccarato · Paolo Calza

Abstract

Purpose A new iterative reconstruction algorithm (WBR™) has been recently proposed for cardiac single photon emission computed tomography (SPECT). The WBR™ technology is designed to reduce noise, improving lesion identification without affecting the image resolution, allowing SPECT studies with reduced count statistic. This allows for either half-time (HT) or half-dose (HD) cardiac SPECT, with image quality and quantitative data comparable to standard-time (ST) or standard-dose (SD) SPECT. Few data exist on the comparison between conventional filtered backprojection (FBP) and this new algorithm in a clinical setting. The aim of this study was to compare the performance of FBP and WBR™.

Methods Phantoms studies were performed to compare spatial resolution and contrast recovery with FBP, ordered subset expectation maximization (OSEM) and WBR™. A group of 92 patients, with different cardiac pathology, scheduled for a stress-rest SPECT were studied: 52 patients (group A) were injected with a SD of tracer and underwent both ST and HT SPECT; 40 patients (group B) were injected with a half dose of tracer and underwent ST SPECT and immediately after an additional SPECT at double time/projection (DT), to compensate for the low count statistic. A 2-day ^{99m}Tc-sestamibi protocol was used in all patients. SD/ST and HD/DT SPECT were reconstructed with a conventional FBP; SD/HT and HD/ST SPECT were reconstructed with WBR™. The summed stress score (SSS) and summed rest score (SRS) were calculated; the left ventricular ejection fraction (LVEF) was automatically derived.

Results In group A (SD), no significant differences were observed between ST FBP SPECT and HT WBR™ in SSS (11.1 and 11.7, respectively) and SRS (9.4 and 10.3, respectively, NS). LVEF on rest acquisitions was also comparable (50% on ST SPECT and 49% on HT SPECT, NS); LVEF on post-stress studies in HT SPECT (46%) was lower than ST SPECT (50%), although not statistically significant. In group B (HD), SSS (6.2 in ST and 5.3 in DT) and SRS (4.0 in ST and 3.3 in DT) were also comparable. No differences were documented between ST and DT in rest (47 and 48%, respectively) and stress (48 and 50%, respectively) LVEF.

Conclusion WBR™ performance and image quality were comparable to those of conventional FBP, allowing for either HT or HD studies. The former allows for an increased patient throughput and optimization of resources. The latter modalities would allow for a significant reduction in both patients' and operators' exposure. Further studies are needed to validate the clinical use of this method.

C. Marcassa (✉)
Cardiology Department, S. Maugeri Fnd, IRCCS,
Scientific Institute of Veruno (NO),
V. Revislate 13,
Veruno, NO, Italy
e-mail: claudio.marcassa@fsm.it

R. Campini · O. Zoccarato · P. Calza
Nuclear Medicine Department, S. Maugeri Fnd, IRCCS,
Scientific Institute of Veruno (NO),
Veruno, Italy

Introduction

Many parameters can affect the image quality of single photon emission computed tomography (SPECT) scans,

including the radiopharmaceutical uptake (lesion to background uptake ratio), physiological factors (such as patient age, size and weight), the acquisition time, injected dose and intrinsic system characteristics such as resolution.

In cardiac SPECT acquisitions, two main factors are involved in the loss of quality of the images: the noise and the characteristics of the collimators. Recently, new iterative algorithms, able to compensate for these factors, have been proposed: Wide Beam Reconstruction (WBR™, Ultraspect, Haifa, Israel), Evolution for Cardiac (GE Medical Systems, Waukesha, WI, USA) and Astonish (Philips Healthcare, Eindhoven, The Netherlands) [1–3].

The WBR™ has been recently proposed for short-time cardiac SPECT [1, 3]. Among the principal characteristics of this algorithm there is the ability to recover the losses of resolution at different source-detector distances. The techniques of resolution recovery applied to iterative algorithms are able to produce images characterized by a better resolution but with a reduction of the signal to noise ratio due to an increased level of noise. To contain the increase in noise, the techniques of resolution recovery include a smoothing post-filter.

Differently from other algorithms, the WBR™ technology does not use a post-filter; it was designed to reduce noise by modelling it from the spectral analysis of the projections, thus improving lesion identification without affecting the image resolution [1, 2]. As a result of the noise suppression and the resolution recovery, the WBR™ allows for substantially shorter scan time without compromising image quality, with a potential increase in patient throughput and optimization of resources in most busy nuclear medicine departments. Alternatively, a reduced amount of injected tracer can be employed, leading to a reduction in patients' as well as personnel's exposure [4, 5]. Moreover, the latter could be helpful in situations of ^{99m}Tc supply shortage.

The aim of this study was to compare the performance of routinely used FBP and WBR™ in phantom studies and in the clinical arena (1) in a group of patients undergoing a half-time (HT) gated SPECT and (2) in a second group of patients injected with a reduced tracer activity.

Materials and methods

Study population and protocol

A group of 92 consecutive patients (age 62±10 years, 57% male), with different cardiac pathology, scheduled for a stress-rest myocardial perfusion study were prospectively studied. Patients with a history of a recent (<30 days) myocardial infarction or recent coronary revascularization were excluded, as well as those with haemodynamically significant valvular disease, pacemaker or atrial fibrillation. All patients gave their informed consent.

Phantom studies

A three-line source phantom was used to evaluate the spatial resolution, according to NEMA standards, with the following parameters: camera equipped with a low-energy high-resolution (LEHR) collimator, pixel size 3.4 mm, angular range 360° with a 3° angular step and 200 mm radius of rotation. The acquisitions were reconstructed with a conventional filtered backprojection (FBP, Butterworth filter: cutoff 0.4 cycle/cm and order 10), an iterative ordered subset expectation maximization (OSEM) algorithm (4 iterations) and by the WBR™ algorithm. No attenuation or scatter correction was applied. The central and peripheral (radial and tangential) resolutions were calculated as full-width at half-maximum (FWHM) of the related linear profile, after Gaussian filtering. A cylindrical phantom with hot and cold spheres, ranging in diameter from 9.5 to 25.4 mm, was used to evaluate the contrast recovery with FBP, OSEM and WBR™. Contrast recovery with hot spheres was calculated as: $CR = \frac{|Sp-Bg|}{Bg}$ where Bg is the average pixel background counts in a circular region of interest (ROI) taken in the centre of the phantom. Using the transaxial image corresponding to the centre of the spheres, the average pixel count (Sp value) was evaluated with a circular ROI centred on the spheres with a diameter equal to half of the sphere diameter. The contrast recovery for the cold spheres was calculated in a similar way.

Stress testing

A 2-day imaging protocol was used; rest and stress scans were obtained in random order, with a 48-h interval. Rest studies were performed on full therapy. In the 61% of patients who were able to achieve >85% of their maximal age-predicted heart rate as documented by a previous exercise test, a multistage symptom-limited exercise test was performed, after an overnight fast and with medications withheld at least 24 h before the test for nitrates and 48 h for beta and calcium channel blockers. A 12-lead ECG was recorded every minute and blood pressure every 3 min. Incremental loads of 25 W were achieved every 3 min, and patients exercised until their maximal predicted heart rate was attained or they complained of exercise-limiting fatigue, chest pain, dyspnoea, hypotension, or until complex arrhythmias or

a downsloping or horizontal ST segment depression >0.25 mV. In the remaining 39% of patients, a dipyridamole test was performed (0.56 mg/kg in 4 min followed by 3 min of low-level exercise) after an overnight fast and with medications withheld at least 12 h before; in particular, the patients were instructed to avoid caffeine-containing drugs and beverages. Sestamibi was injected at peak exercise or 2 min after the end of dipyridamole infusion. For both exercise and dipyrida-mole tests, the ECG response was defined as positive for ischaemia if there was horizontal or downsloping ST segment depression > 0.1 mV for >80 ms after the J point and for at least 3 consecutive beats.

Sestamibi image acquisition and processing

After the tracer injection, a light meal was provided to accelerate the hepatobiliary clearance of the tracer and to improve the heart to background ratio. Images were acquired 45–60 min after the tracer injection. All patients performed an 8 bin/cycle ECG-gated SPECT acquisition

with a dual-head camera at 90°, equipped with a LEHR collimator, on a 64×64 matrix and a pixel size of 6.9 mm, over a 180° arc starting from the 45° right anterior oblique projection. Particular care was taken to avoid major artefacts, such as patient motion during acquisition.

Group A: patients were injected with a standard dose of tracer, according to the EANM/ESC proce-dural guidelines for myocardial perfusion imaging in nuclear cardiology (9 MBq/kg, standard dose, SD) [6]. A standard ECG-gated SPECT acquisition with 30 projections/head and a time/projection of 20 s was first performed (600 s acquisition time, standard time, ST). Immediately after the conclusion of the acquisition, a second ECG-gated acquisi-tion was performed at half time/frame (10 s/projection, 300 s acquisition time, HT). ST SPECT was reconstructed with a conventional FBP algorithm using a Butterworth filter (cutoff 0.4 cycle/cm and order 10). HT SPECT was reconstructed with the new WBR™ algorithm. No attenuation or scatter correction was performed.
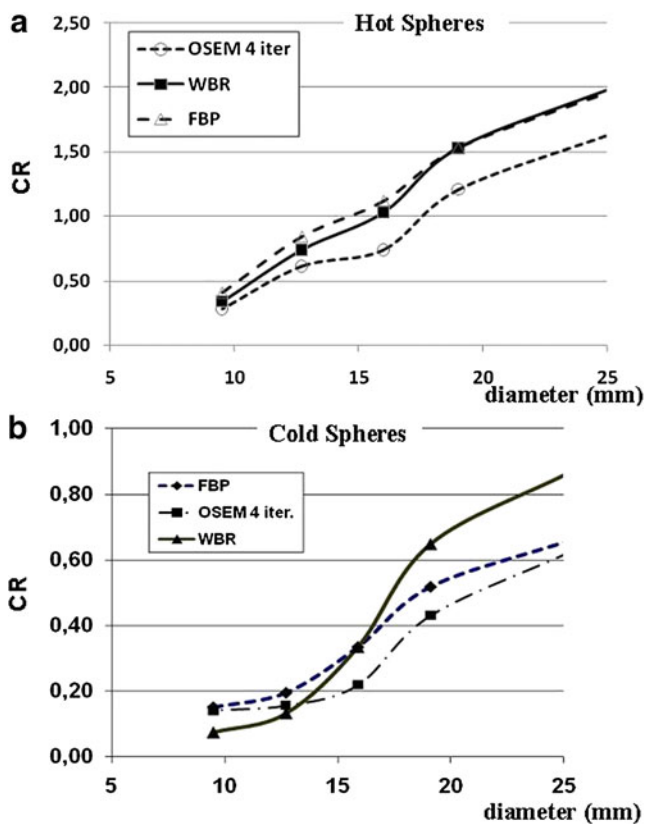
Fig. 1 Contrast recovery curves as function of spheres' diameters in a hot (**a**) and cold (**b**) spheres phantom, with FBP, OSEM and WBR™. In the hot spheres phantom, (**a**), WBR™ and FBP showed a better contrast recovery over OSEM. In the cold spheres phantom, (**b**), WBR™ contrast recovery curve showed a better dynamic range compared to OSEM and FBP
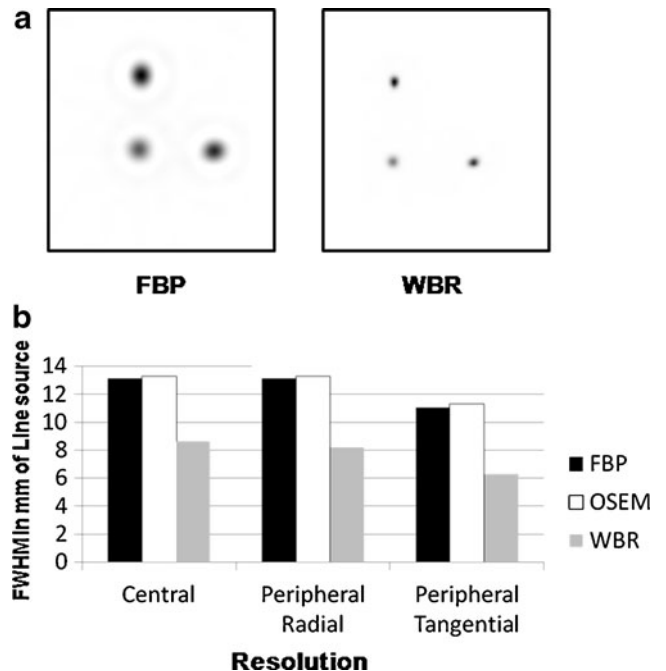
Fig. 2 Representative images of the three-line source phantom reconstructed with FBP (**a**, *left*) and WBR™ (**a**, *right*), and central and peripheral (radial and tangential) resolution, calculated as FWHM on the line source profile (**b**). A clear improvement in resolution with WBR™ (*grey bars*) over FBP (*black bars*) and OSEM (*white bars*) was documented

Table 1 Clinical characteristics of the study cohort

	Group A	Group B
Age (years)	61±11	63±10
Gender (M:F) (%)	54:46	61:49
Previous myocardial infarction (%)	42	39
Effort chest pain (%)	35	28
Previous revascularization (CABG or PTCA) (%)	44	41
Type of test (%)		
Exercise	62	60
Dypiridamole	38	40

CABG coronary artery bypass grafting, *PTCA* percutaneous coronary angioplasty

Group B: patients were injected with half the standard dose of tracer (4.5 MBq/kg, half dose, HD). A standard acquisition with a time/frame of 20 s was first performed. Immediately after the conclusion of the acquisition, a second ECG-gated acquisition was performed at double time/frame (40 s, DT), in order to obtain count statistics comparable to those of a conventional SD ST study. ST SPECT was reconstructed with the WBR™ algorithm. DT SPECT was reconstructed with a conventional FBP algorithm using a Butterworth filter (cutoff 0.4 cycle/cm and order 10). No attenuation or scatter correction was performed.

Image analysis

The myocardial regional tracer uptake was evaluated by two blinded experienced observers in 17 segments, with a 5-point scoring system (from 0 = normal to 4 = absent). Discrepancies were resolved by consensus. Summed stress scores (SSS) and summed rest scores (SRS) were calculated. A stress study was defined as normal when SSS <3; the presence of ischaemia was defined as a summed difference score (SDS) >1. The left

ventricular ejection fraction (LVEF) was automatically calculated with the Quantitative Gated SPECT software (QGS, Cedars-Sinai Medical Center, Los Angeles, CA, USA) [7] in both studies. The quality of each study was graded on a 4-point scale (from 3 = optimal to 0 = inadequate).

Statistical analysis

Data are reported as mean±SD. SD/ST and SD/HT data were compared using Student's *t* test for paired data, as well as HD/ST and HD/DT data. Categories were compared with the chi-square test. The correlation between SD/ST and SD/HT and between HD/ST and HD/DT perfusion and function results was evaluated by linear regression analysis; data were also analysed according to the method of Bland and Altman [8]. A *p* value <0.05 (two-tailed) was considered significant.

Results

Contrast recovery and spatial resolution

The contrast recovery curves in the hot and cold spheres phantom for FBP, OSEM and WBR™ are reported in Fig. 1. In the hot spheres phantom, for the different spheres' diameters, WBR™ and FBP showed a better contrast recovery over OSEM. In the cold spheres phantom, the WBR™ contrast recovery curve showed a better dynamic range compared to OSEM and FBP. The central and peripheral (radial and tangential) resolution in NEMA conditions for SPECT studies reconstructed with FBP, OSEM and WBR™ are reported in Fig. 2; a clear improvement in resolution was documented for WBR™ over FBP and OSEM.

Clinical results

The clinical characteristics of the study cohort are reported in Table 1.

Table 2 Perfusion scores and functional data in ST and HT SPECT in group A patients

	ST (FBP reconstruction)	HT (WBR™ reconstruction)	*p* value
Stress SPECT total counts	7.4×10⁶	3.3×10⁶	<0.0001
Rest SPECT total counts	7.2×10⁶	3.1×10⁶	<0.0001
SSS	11.1±15.3	11.7±16.1	NS
SRS	9.4±15.6	10.3±16.2	NS
Normal stress studies (%)	26 (50%)	27 (51%)	NS
Reversible ischaemia (%)	14 (28%)	16 (31%)	NS
Stress LVEF (%)	50±15	46±16	NS
Rest LVEF (%)	50±16	49±16	NS

**Table 3** Perfusion scores and functional data in ST and DT SPECT in group B patients

|	ST/HD (WBR™ reconstruction)	DT/HD (FBP reconstruction)	p value
Stress SPECT total counts	3.2×10^6	6.8×10^6	<0.0001
Rest SPECT total counts	3.3×10^6	7.0×10^6	<0.0001
SSS	6.2±9	5.3±9	NS
SRS	4.0±9	3.3±8	NS
Normal stress studies (%)	23 (58%)	23 (58%)	NS
Reversible ischaemia (%)	13 (32%)	14 (36%)	NS
Stress LVEF (%)	48±11	50±12	NS
Rest LVEF (%)	47±13	48±13	NS

Quality of the study

Group A: ST studies collected on average 7.2×10^6 and 7.4×10^6 counts at rest and stress, respectively, and HT studies collected on average 3.1×10^6 and 3.3×10^6 counts at rest and stress, respectively (44% of ST studies). The image quality was comparable between ST and HT acquisitions (average quality score 2.1±0.2 and 2.1±0.3, respectively, NS); in particular, the quality of the study was graded as good-optimal in 87% in ST and 86% in HT studies, respectively (NS), and no study was graded as inadequate.

Group B: ST studies collected on average 3.3×10^6 and 3.2×10^6 counts at rest and stress, respectively, and DT studies collected on average 7.0×10^6 and 6.8×10^6 counts at rest and stress, respectively. The image quality was comparable between ST and DT acquisitions (average quality score 2.0±0.3 and 2.1±0.3, respectively, NS); in particular, the quality of the study was graded as good-optimal in 86% in ST and 85% in DT studies, respectively (NS), and no study was graded as inadequate.

Fig. 3 Linear correlation between ST SPECT (x-axis) and HT SPECT (y-axis) for standard-dose studies, for the SSS (**a**), the SRS (**b**), the post-stress LVEF (**c**) and the rest LVEF (**d**) in group A. A very high correlation was documented
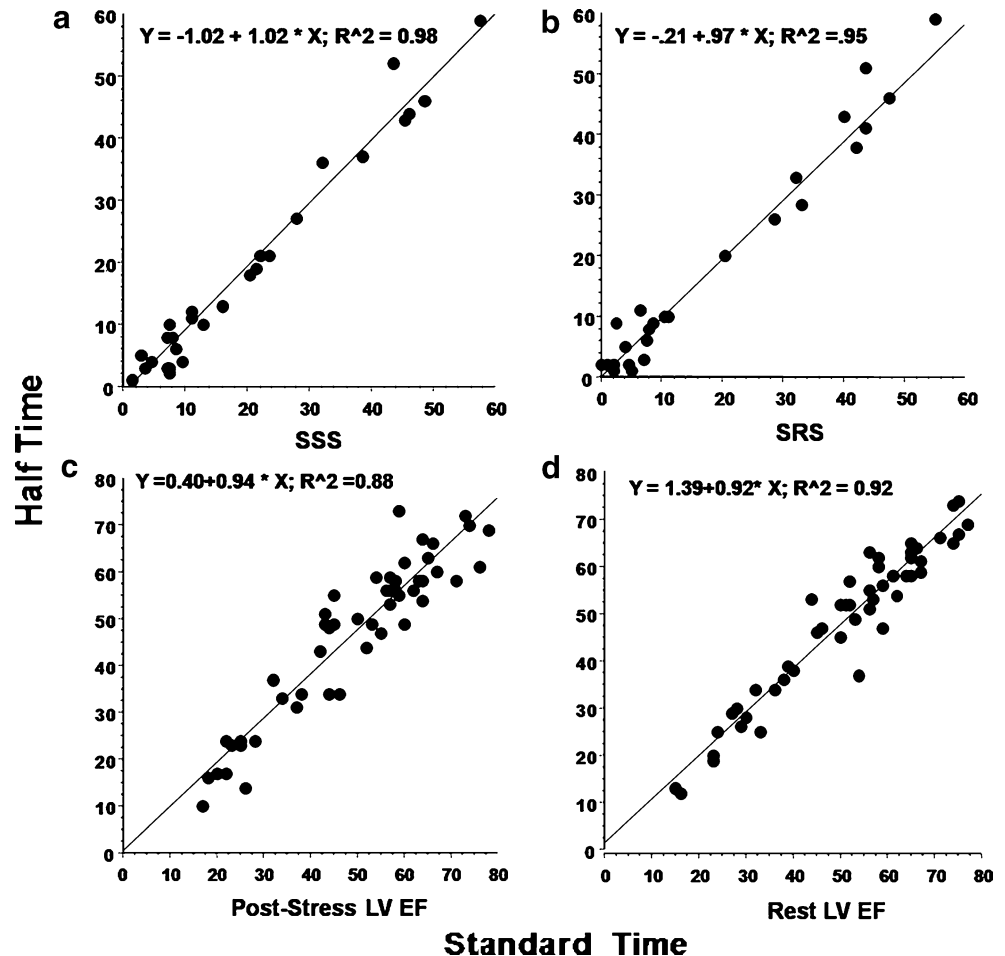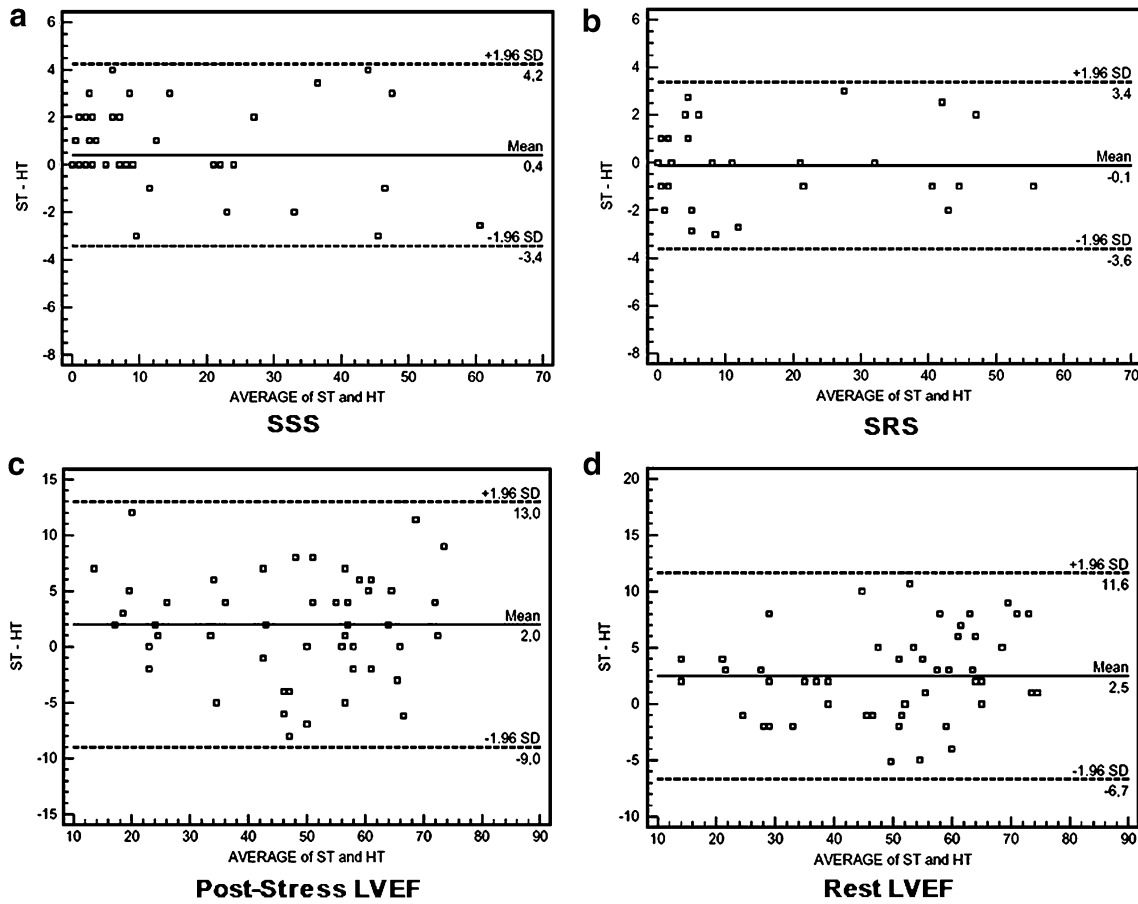
Fig. 4 Bland-Altman plot of ST versus HT standard-dose SPECT for the SSS (**a**), the SRS (**b**), the post-stress LVEF (**c**) and the rest LVEF (**d**) in group A. All individual differences in data points did fall within 1.96 SDs of the overall average differences between the two methods, indicating no clinical differences between the two methods

Fig. 5 Linear correlation between ST SPECT (x-axis) and ST SPECT (y-axis) for half-dose studies, for the SSS (**a**) the SRS (**b**), the post-stress LVEF (**c**) and the rest LVEF (**d**) in group B. A very high correlation was documented
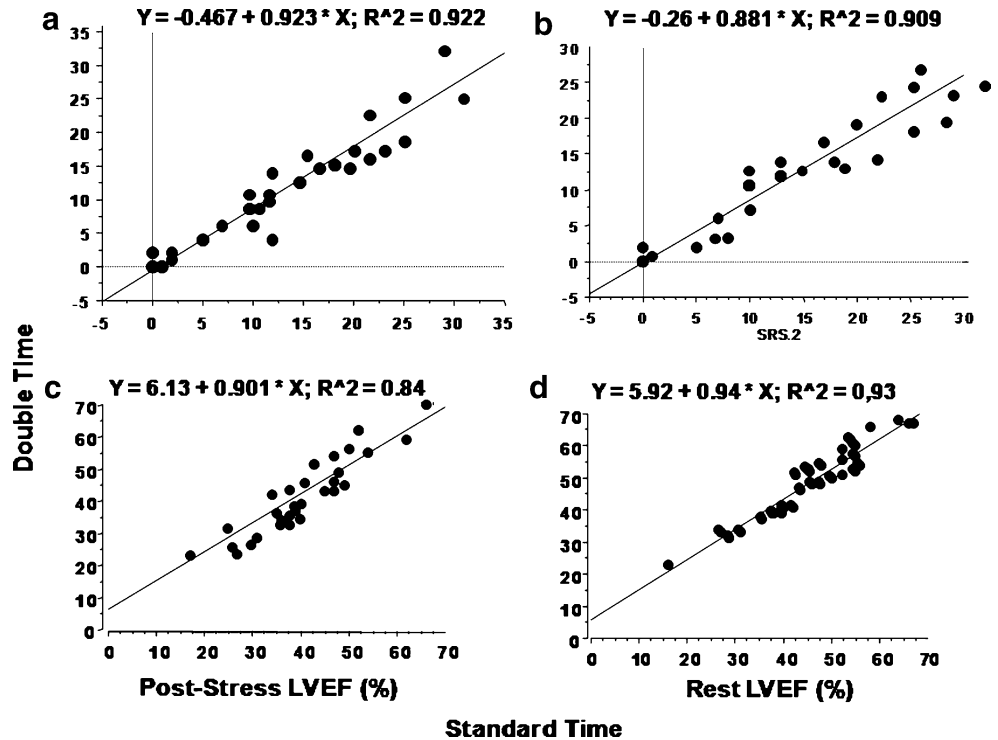
Perfusion results and study interpretation

Group A: no significant differences were observed between ST FBP SPECT and HT WBR™ SPECT in SSS (11.1±15.3 and 11.7±16.1, respectively, NS) and SRS (9.4±15.6, and 10.3±16.2, respectively, NS). According to the SSS, stress images were classified as normal in 26 patients on ST (50%) and in 27 patients on HT SPECT (51%, NS). According to the SDS, ischaemia was identified in 14 patients on ST (28%) and in 16 patients on HT SPECT (31%, NS). The agreement between ST and HT SPECT was 91% (κ=0.77) in the correct classification of stress images and 88.% in the detection of ischaemia (κ=0.72). *Group B*: in group B, SSS (6.2 in ST and 5.3 in DT) and SRS (4.0 in ST and 3.3 in DT) were also comparable between the two acquisitions. According to the SSS, stress images were classified as normal in 23 patients (58%) either on ST or DT SPECT. According to the SDS, ischaemia was identified in 13 patients on ST (32%) and in 14 patients on DT SPECT (36%, NS). The agreement between ST and DT SPECT was 95% (κ=0.89) in the correct classification of stress images and 88% in the detection of ischaemia (κ=0.78).

Functional results

In group A, the average LVEF on rest studies was comparable between the two sets of acquisitions (50±16% on ST vs 49±16% on HT gated SPECT, NS). LVEF on post-stress studies in HT gated SPECT (46±16%) was lower than ST gated SPECT (50±15%), although the difference was not statistically significant. In group B, no differences were documented between ST and DT LVEF both on rest (47 and 48%, respectively) and stress (48 and 50%, respectively) studies. Perfusion and functional results in group A and in group B are reported in Tables 2 and 3, respectively.

Correlation between FBP and WBR™ data

In group A, very high correlation between SSS, SRS, stress and rest LVEF on ST and HT images was documented by linear regression analysis (Fig. 1). The Bland-Altman plots for SSS, SRS, LVEF on rest and stress acquisitions are reported in Fig. 2. In group B, a very high correlation between SSS, SRS, stress and rest LVEF at ST and HT
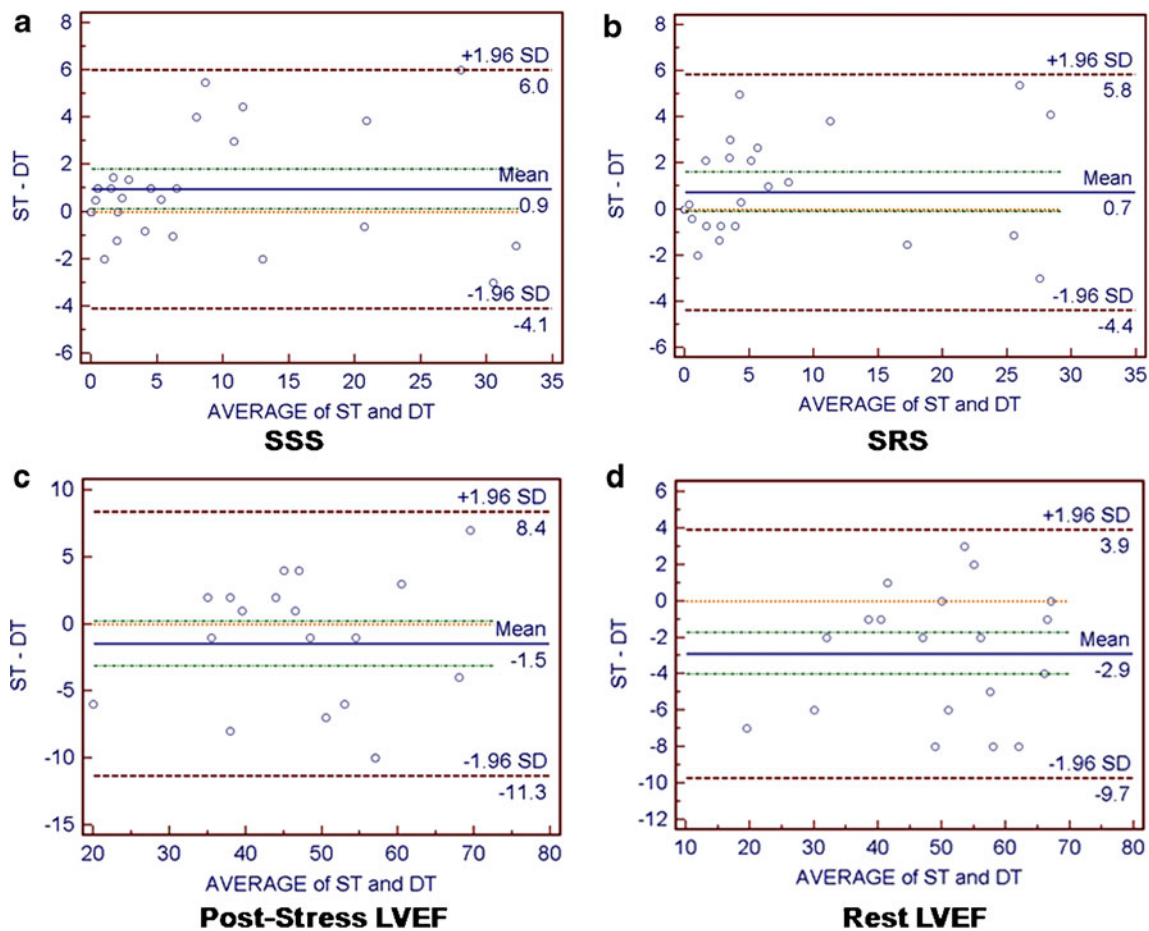
Fig. 6 Bland-Altman plot of DT versus ST half-dose SPECT for the SSS (**a**), the SRS (**b**), the post-stress LVEF (**c**) and the rest LVEF (**d**) in group B. All individual differences in data points did fall within 1.96 SDs of the overall average differences between the two methods, indicating no clinical differences between the two methods

SPECT was also documented by linear regression analysis (Fig. 3). The Bland-Altman plots for SSS, SRS, LVEF on rest and stress acquisitions in group B are reported in Fig. 4 (see also Fig. 5, Fig. 6, Fig. 7).

Discussion

The results of the present study demonstrate that image quality, quantitative functional results and interpretation of HT gated SPECT or HD gated SPECT reconstructed with the new algorithm WBR™ were comparable to those of ST gated SPECT or DT gated SPECT acquisition reconstructed with conventional FBP. In group A, differences in the time elapsed from the end of the stress test and the SPECT acquisition could be involved and explain the small differences of LVEF between the two post-stress studies.

We documented, in phantom studies, the quantitative advantages of the WBR™ method over OSEM and
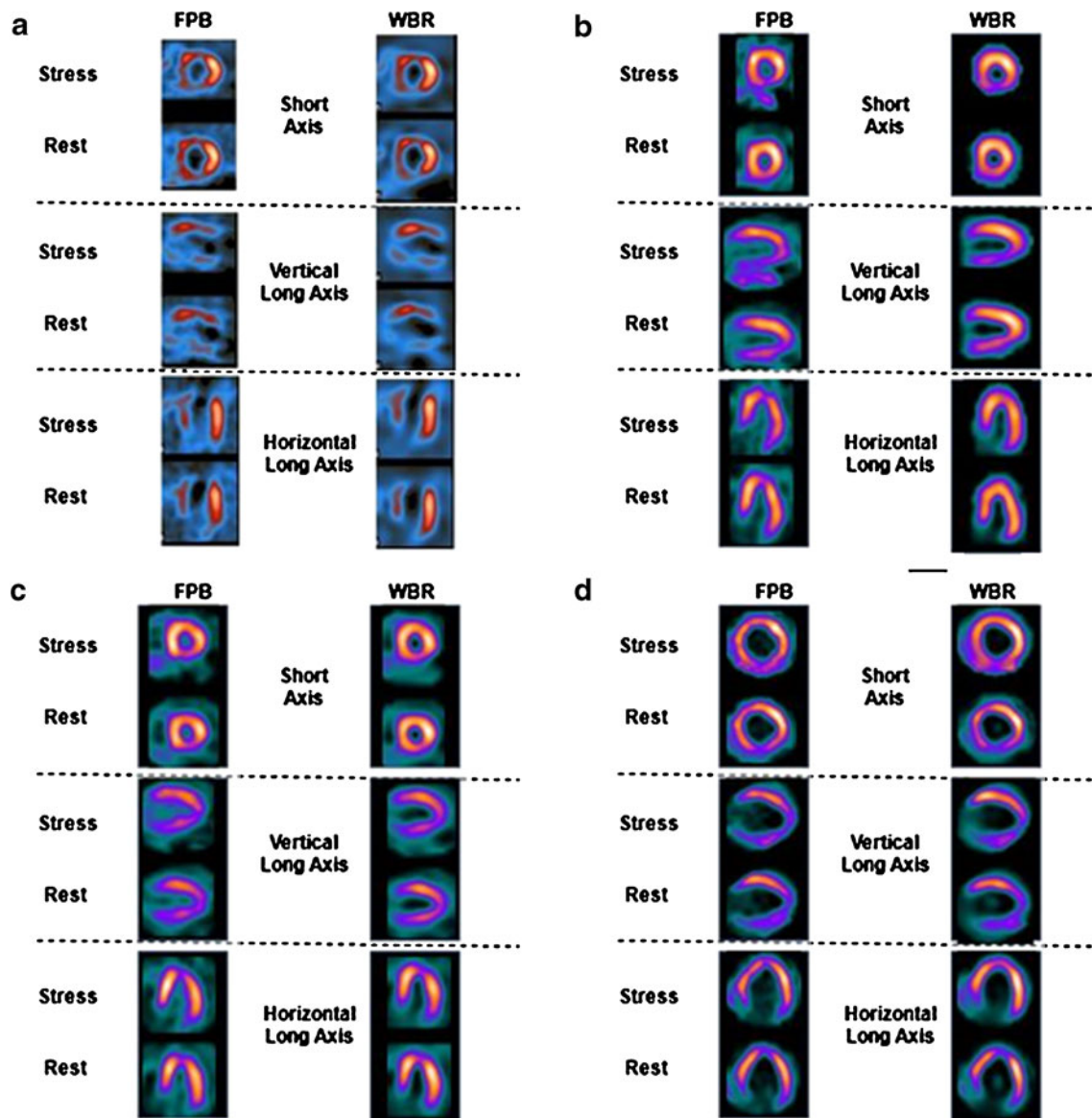
Fig. 7 Stress-rest mid-ventricular axis of three representative patients with ischaemic heart disease (**a**–**c**) reconstructed with FBP after the ST acquisition and with WBR™ after the HT acquisition. **d** Images of a patient with dilated cardiomyopathy reconstructed with WBR™, after injection of a half dose of tracer and ST acquisition, or DT acquisition reconstructed with FBP are shown. **a** Severe perfusion defects in anterior, apical and inferior walls are documented. **b** Mild inferior ischaemia is shown. **c** A patient with no perfusion defects is shown. **d** Mild fixed perfusion defects in inferior and apical regions in a patient with dilated cardiomyopathy are reported. In all cases, the image quality is comparable between the different reconstruction methods

conventional FBP reconstruction [9–11]. In particular, a better image contrast, without an increase in background noise, was obtained in both hot and cold sphere phantoms, and in an anthropomorphic cardiac phantom with simulated cold lesions in different positions [9–11]. Our phantom results are comparable to those previously obtained by other authors [1].

Using half of the standard scan time, with an administered activity as recommended by the EANM/ESC procedural guidelines for myocardial perfusion imaging in nuclear cardiology [6], the present study demonstrates that images may be obtained with qualitative and quantitative results comparable to studies performed according to guideline recommendations [6]. Our results are comparable to those of other clinical investigations [1, 2]. In addition, we also confirm preliminary evidence that HD gated SPECT studies are also feasible, with qualitative and quantitative data comparable to studies with standard count statistics [5].

The cornerstone of WBR™ reconstruction technology is an iterative reconstruction technique where the main physical events of a scintigraphic detection process are modelled. The model compensates for non-stationarity of the collimator's response ("beam spread function" effect); corrects for variation of the detector-patient distance; utilizes all of the collimator parameters that affect the line spread function; takes into consideration the statistical behaviour of the emission and noise which may vary from one application to the other; incorporates attenuation maps and scatter models (not evaluated here); and is operator independent [1].

Acquisitions at half time/frame approximately collected half total counts than standard time/frame acquisitions. On a theoretical basis, such a low photon count may be obtained also with a standard time/frame acquisition but with half of the standard dose/patient injected. According to this hypothesis, as a matter of fact, in our group B patients ST gated SPECT total counts were comparable to those of group A HT acquisitions.

The possibility to obtain good qualitative studies with a reduced amount of injected tracer would allow one to significantly reduce patients' effective dose to 4.9–6.5 mSv for a stress-rest study with a Tc-labelled tracer, a value comparable to that from a conventional X-ray angiogram (2–6 mSv) and less than that from multidetector CT coronary angiography (6–15 mSv) [12]. Operators' exposure will be significantly reduced as well. Moreover, the possibility to perform gated SPECT studies with reduced tracer activities will allow one to face the periods of shortage of ^{99m}Tc, due to the shutdown of nuclear reactors for maintenance. Furthermore, it will give a consistent answer to the request for dose containment to the population (taking into consideration also the introduction of the new CT methods in nuclear medicine).

Limitations of the study

No comparison was performed between ST and HT gated SPECT or SD and HD gated SPECT in terms of sensitivity and specificity for coronary stenoses; however, the aim of the study was to compare WBR™-reconstructed low count SPECT with standard SPECT in terms of image quality, interpretation and functional results. Finally, no attenuation or scatter correction was performed, and additional experimental and clinical studies are required.

Conclusion

WBR™ performance was comparable to that of conventional FBP SPECT, with an image quality comparable to that of standard gated SPECT studies, thus allowing for either half-time or half-dose studies. The former allows for an increased patient throughput and optimization of resources. The latter modalities will be probably more effective, since they involve different aspects of nuclear medicine practices, both of sanitary and economic nature, including the reduction of the dose to the patients as well as to the operators and the population, and a better management of the reduced availability of ^{99m}Tc.

Conflicts of interest None.

References

1. Borges-Neto S, Pagnanelli RA, Shaw LK, Honeycutt E, Shwartz SC, Adams GL, et al. Clinical results of a novel wide beam reconstruction method for shortening scan time of Tc-99m cardiac SPECT perfusion studies. J Nucl Cardiol 2007;14:555–65.
2. Venero CV, Heller GV, Bateman TM, McGhie AI, Ahlberg AW, Courter D, et al. A multicenter evaluation of a new post-processing method with depth-dependent collimator resolution applied to full-time and half-time acquisitions without and with simultaneously acquired attenuation correction. J Nucl Cardiol 2009;16:714–25.
3. DePuey EG, Bommireddipalli S, Clark J, Thompson L, Srour Y. Wide beam reconstruction "quarter-time" gated myocardial perfusion SPECT functional imaging: a comparison to "full-time" ordered subset expectation maximum. J Nucl Cardiol 2009;16:736–52.
4. Marcassa C, Campini R, Zoccarato O, Calza P. Wide beam reconstruction for gated-SPECT: going toward optimization of resources and reduction in radiation exposure. Eur J Nucl Med Mol Imaging 2008;35(Suppl 2):S251.
5. DePuey G, Bommireddipalli S. Half-dose myocardial perfusion SPECT with wide beam reconstruction. Circulation 2009;120: S334
6. Hesse B, Tägil K, Cuocolo A, Anagnostopoulos C, Bardiés M, Bax J, et al. EANM/ESC procedural guidelines for myocardial perfusion imaging in nuclear cardiology. Eur J Nucl Med Mol Imaging 2005;32(7):855–97.

7. Germano G, Kiat H, Kavanagh PB, Moriel M, Mazzanti M, Su HT, et al. Automatic quantification of ejection fraction from gated myocardial perfusion SPECT. J Nucl Med 1995;36:2138–47.

8. Bland JM, Altman DG. Statistical methods for assessing agreement between two methods of clinical measurements. Lancet 1986;1(8476):307–10.

9. Zoccarato O, Campini R, Marcassa C, Calza P. Comparison between filtered back projection SPECT reconstruction and a new iterative reconstruction algorithm: a phantom study. Eur J Nucl Med Mol Imaging 2007;34(Suppl 2):S237.

10. Zoccarato O, Campini R, Marcassa C, Calza P. Comparison between filtered back projection SPECT reconstruction and a new iterative reconstruction algorithm: an anthropomorphic cardiac phantom study. Eur J Nucl Med Mol Imaging 2007;34(Suppl 2):S280.

11. Zoccarato O, Campini R, Marcassa C, Calza P. Performance of a new iterative reconstruction algorithm for cardiac short-time SPECT: preliminary results in an anthropomorphic cardiac phantom study. Comput Cardiol 2008;35:329–332.

12. Marcassa C, Bax JJ, Bengel F, Hesse B, Petersen L, Reyes E, et al. Clinical value, cost-effectiveness, and safety of myocardial perfusion scintigraphy: a position statement. Eur Heart J 2008;29:557–63.